

MECHANICAL PROPERTIES OF THERMOPLASTIC POLYMERS 3D PRINTED IN A LOW VACUUM ENVIRONMENT

Aurelian ZAPCIU^{1,*}, George CONSTANTIN²

¹⁾ Eng., PhD Student, Faculty of Industrial Engineering and Robotics, University "Politehnica" of Bucharest, Bucharest, Romania

²⁾ Prof. Dr. Eng., Industrial Engineering and Robotics Faculty, University "Politehnica" of Bucharest, Romania

Abstract: 3D Printing with high processing temperature polymers brings challenges due to the exposure of the printed part to ambient air convection leading to thermal stresses inside the part and improper interlayer adhesion. This results in parts that have inferior mechanical properties compared to other manufacturing methods. This paper presents a method of improving printability and mechanical properties of parts from high processing temperature polymers by eliminating or drastically reducing the impact of ambient air with the use of a low-vacuum printing chamber. Tests parts were printed in a specially-designed 3D printer with an enclosed, vacuum sealed printing chamber. The air inside the print chamber was evacuated before the printing process begins. Specimens made from polyetherimide (PEI - ULTEM 1010) showed a 14% increase in strength when printed in a low-vacuum environment, using the same process parameters, while specimens made from acrylonitrile styrene acrylate (ASA) did not show significant differences. Additionally, surface quality was investigated using atomic force microscopy showing the method did not produce significant changes in surface roughness. Neither did the thermal behavior of 3D printed parts investigated using differential scanning calorimetry. The results point to removal of the convective thermal transfer during the 3D printing process having an overall positive effect on mechanical properties.

Key words: 3D Printing, vacuum chamber, engineering plastics, FDM, polyetherimide.

1. INTRODUCTION

Additive manufacturing (AM) is the current term used for what was previously called rapid prototyping and what is commonly called 3D printing. The term rapid prototyping is used in a variety of industries to describe a process for the rapid creation of a physical model of a part or system prior to commercialization. The constant improvement of the results obtained by applying rapid prototyping technologies has allowed the obtaining of models with a functional role, with characteristics closer to those of final products made through other fabrication methods. Today, AM is a growing industry forecast to expand by double digit compound annual growth through 2028 [1]. The basic principle of AM technology is that a virtual model, generated using 3D CAD technologies, can be manufactured directly, without the need to plan a manufacturing process. Thus, FA technology allows the simplification of the processes of obtaining complex three-dimensional objects directly from virtual CAD models. FA works by adding material in layers, each layer of material being a section of the part obtained from the CAD model. Since the layers have a certain thickness, the resulting piece is an approximation of the digital model. The thinner the material layers, the closer the resulting piece will be to the digital model. To date,

all additive manufacturing machines marketed use layer-by-layer manufacturing processes, and the major differences between the processes used in FA are specifically related to the materials used and the way the layers of material are fused. These differences lead to major characteristics of the final parts, such as dimensional accuracy, material properties and mechanical properties but also characteristics related to the manufacturing process, for example duration of manufacture, the need for post-processing operations of the part, dimensions of the FA machine, the cost of the machine, materials or manufacturing process.

The FDM process was first marketed by Stratasys in 1991, with patents being granted to the company's founder, Scott Crump in 1992. The machines sold by Stratasys were well received, as the manufacturing process and mechanical structure of the machines were low cost compared to those using stereolithography, but the explosion in popularity of the FDM process came with the expiration of the patents held in the field.

The process produces parts by extruding a material, usually a thermoplastic polymer. The extruder pushes a filament of thermoplastic material through a heated nozzle moving in the XY plane to create a two-dimensional layer. This layer is a section of the digital model of the solid to be manufactured. To ensure proper fusion between the layers of material, the base (called a printing bed or build platform) on which the first layer is deposited or the machine enclosure is heated.

Where necessary, support material can be deposited using a separate nozzle. The support structures will be

* Corresponding author: Splaiul Independenței 313, 060042, Bucharest, Romania,
Tel.: (+40) 021 402 9174,
E-mail addresses: aurelianzapciu@yahoo.com (A. Zapciu).

removed by various methods after completion of the fabrication process. The precision and accuracy of the process are limited by the size of the nozzle, which can have diameters of tenths of millimeters.

Material extrusion 3D printing (ME3DP) is the non-trademarked process equivalent to Stratasys' FDM. This process produces layered polymer parts with complex geometry but with mechanical properties worse than those of parts made with other technologies, such as injection molding. Following the expiration of patents held by Stratasys in 2009, ME3DP has seen widespread adoption, with the technology being adopted by manufacturers that created products for home users, public institutions and businesses of all sizes [2].

Parts fabricated using ME3DP have inherent flaws stemming from the layered aspect of the process, as well as from the gradual aspect of material deposition. After polymer material is extruded through the heated nozzle of a 3D printing machine, it begins cooling down through convective thermal interaction with the atmospheric air and through thermal conduction with the previously deposited material. When the next layer of material is being deposited, the underlying layer begins reheating briefly, in contact with the higher temperature polymer. This repeated cooling and heating results in internal thermal stresses developing in the part [3], leading to reduced mechanical properties compared to injection molding processes [4]. More so, because of the significant thermal cooling following extrusion, the adhesion between successive layers may be insufficient. This is also present in the deposited adjacent filaments, but to a lesser extent. For this reason, 3D printed parts exhibit an anisotropic behavior where the mechanical properties on the Z axis (perpendicular to the build platform) are inferior to those on the X and Y axis (parallel to the build platform) [5].

These effects cause a series of issues when processing high temperature thermoplastics such as polyetherimides, polyaryletherketones or polyphenylsulfones [6], to name a few. To a lesser extent, the problems also appear in thermoplastic polymers with high thermal expansion coefficients such as ABS (acrylonitrile butadiene styrene) [7].

In search of solutions to the problem of printing parts with good mechanical characteristics, different companies have had different approaches. The Polish company Zortrax produces a line of 3D printers without closed enclosure (Zortrax M200, M300) but has developed its own range of thermoplastic materials (Z-Glass, Z-UltraT), with mechanical characteristics superior to those of the common materials (ABS, PLA).

The American company Stratasys uses industrial AM machines that can process thermoplastics with high melting temperatures that have a type of closed enclosure, heated to temperatures between 70 °C, for printers for the manufacture of ABS parts and 90 °C for the Fortus range of printers, with capabilities to produce polyetherimide (PEI) or polyether-ether-ketone (PEEK) parts. Research on parts made of ABS and polyamides in an inert nitrogen medium [8], shows that the mechanical properties of printed parts are better in the absence of oxygen.

Another approach to the problem of using thermoplastic materials with high melting temperatures may be to eliminate the cause of inadequate cooling of the deposited material, namely the phenomenon of thermal convection [9]. This would be possible by depositing molten filament in a vacuum chamber. Thus, the application chosen for detailed investigation in this study is the 3D printing of parts in the absence of atmospheric air, in a sealed, low-vacuum chamber. The exclusion of air aims to uniformize the process of heat transfer from and within the 3D printed part during manufacture, in order to reduce the influence of repeated cooling / heating cycles inherent to the fabrication process on the mechanical properties of the final part.

2. MATERIALS AND METHODS

Since in vacuum chambers the atmospheric air that constitutes the heat convection propagation medium is evacuated, the phenomenon of convective heat transfer is gradually eliminated. After eliminating thermal convection, the temperature transfer in vacuum is done predominantly through thermal conductivity. In the case of an additive manufacturing by fused filament deposition process, two distinct aspects can be identified related to heat transfer, namely: thermal conductivity and heat transfer from the heated extrusion head into the filament and into the body of the extruder when the thermoplastic filament melts, and thermal conductivity and heat transfer from the volume of extruded material in the machine build platform.

Plastics are generally avoided in vacuum applications due to the high degassing rate compared to metallic materials. Like any other material, the surface of plastics is covered by a layer of adsorbed water that must be pumped out of the vacuum chamber. The porous nature of plastic surfaces, as well as their chemical composition make it difficult to drain water from the material. In the case of certain hydroscopic plastics, water molecules can penetrate inside the material. In order to be able to evacuate these water molecules, they must first be brought, by diffusion, to the surface of the material, which requires a long period of evacuation. The plastic itself can be a source of exhaust gases in the form of unpolymerized monomers, plasticizers, stabilizers or other additives. By evaporation during the process of evacuation of the vacuum chamber, these substances can condense on the internal components, contaminating sensitive surfaces [10]. As mentioned above, it is recommended that the walls of a vacuum chamber to be made of metal or non-metal alloys. Due to its good strength, machinability and weldability characteristics, EN-AW-5083 aluminum alloy was chosen for fabrication of the sealed chamber. To size the thickness of the chamber walls, a finite element analysis was performed using the module integrated in Autodesk Fusion 360.

For the purpose of this experiment, a 3D printer with a vacuum-sealed aluminum printing chamber was manufactured and used to fabricate test parts (Fig. 1). The 3D printer uses a Cartesian setup with exterior-mounted stepper motors and internal belt drive. The motion is transferred into the sealed chamber using mechanical feedthroughs.

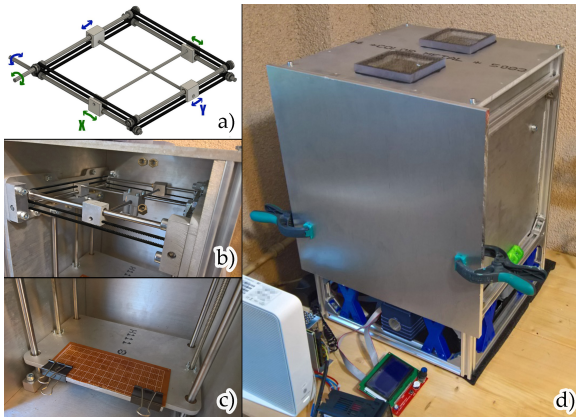


Fig. 1. 3D printer with sealed build chamber: *a, b* – horizontal movement axis; *c* – build platform and vertical movement axis; *d* – 3D printer.

The first aspect considered when designing the printer is the volume occupied by the mechanical structure of the movement system. The working space of the machine must be large enough to allow the manufacture of standard ASTM D638 samples used for destructive testing. A workspace of $180 \times 180 \times 180$ mm was thus established. The volume occupied by the mechanical structure must be minimal, in order to reduce the forces acting on the walls of the enclosure, due to the pressure difference. To meet this criterion, the build platform is fixed in the horizontal plane. The relative movement of the extruder in the horizontal plane is performed using two belt driven axis forming a double portal system. The relative movement in the vertical plane is achieved by translating the build platform on the vertical axis.

A second aspect is the positioning of the stepper motors and other electronics outside the vacuum enclosure and the transmission of the rotational movement through the enclosure wall (Fig. 2). The sealing of the rotating shaft is done with a rotary seal made of fluoropolymer material with low coefficient of friction and high wear resistance. The seal is optimized for vacuum applications, with an elliptical spring forming a pretension force on the inner shaft.

A two-stage vacuum pump connected to the chamber is used to lower the pressure inside the printing chamber. A liquid-cooled, all metal stainless steel extruder head is used for extrusion, as the process temperatures exceed the maximum operation of standard extrusion heads that have an integrated heat-break made of polytetrafluoroethylene. For the build surface, a perforated FR4 board is used. This material allows extruded molten polymer to flow through the perfboard vias, forming a mechanical connection to the build platform.

Two materials were selected for testing the device and the manufacturing method: ASA (acrylonitrile styrene acrylate) and PEI (polyetherimide).

ASA is a thermoplastic material produced as an alternative to ABS (acrylonitrile butadiene styrene) and is widely used in the automotive industry. Structurally, ASA is very similar to ABS but is more resistant to weather and ultraviolet radiation, to long-term high

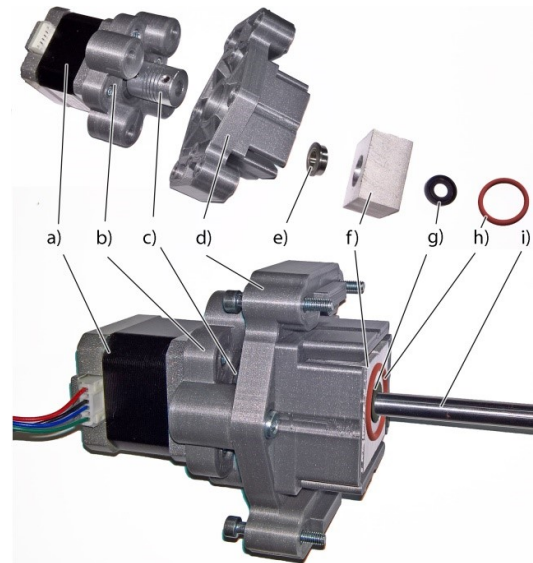


Fig. 2. Motion transmission through vacuum chamber wall (*a* – stepper motor; *b* – motor mounting plate; *c* – elastic coupling; *d* – wall mounting plate; *e* – bearing; *f* – bearing housing; *g* – vacuum seal; *h* – o-ring; *i* – steel shaft).

temperatures and more resistant to alcohols and cleaning agents. ASA retains its gloss, color and mechanical properties when exposed to open air. It has good chemical and thermal resistance, high gloss, good antistatic properties and is hard and rigid. It is used in applications that require weather resistance, such as commercial displays, vehicle exteriors or outdoor furniture.

ASA filament with a diameter of $\varnothing 1.75$ mm sold under the ApolloX brand was acquired commercially from Formfutura (Nijmegen, the Netherlands).

PEI – polyetherimide – is a thermoplastic material with high melting temperature, used especially in food, chemical and medical instruments due to its chemical stability, resistance to solvents and fire and due to the possibilities of sterilization. Ultem is a family of polyetherimides created in the early 1980s by Joseph G. Wirth. ULTEM 1000 (standard resin, without additives) has high dielectric strength, does not burn and emits very little smoke. ULTEM products can be processed by cutting, have very good mechanical properties (strength, rigidity) and can be used continuously at temperatures up to 170 °C.

PEI filament with a diameter of $\varnothing 1.75$ mm sold under the brand Thermax was purchased commercially from 3DXTech (Grand Rapids, MI, USA). The resin from which the filament was made is sold under the brand ULTEM 1010 by SABIC (Riyadh, Saudi Arabia).

The dimensions of the test pieces were chosen according to the testing standard for plastics ASTM D638 type I [11]. The minimum section of the sample is 3.5×13 mm.

Extrusion temperatures for the build materials were set according to the recommendations of the suppliers. A total of 12 fully filled specimens were manufactured, 3 for each material and environmental conditions (atmosphere / vacuum). The process parameters are presented in Table 1.

Table 1

3D printing process parameters

Material	Pressure	Extrusion temp. [°C]	Layer Height	Nozzle
ASA	1 atm	250	0.2 mm	0.4 mm
	15 Pa			
PEI	1 atm	375	0.2 mm	0.4 mm
	15 Pa			

Due to the large difference between the melting temperatures of the two materials, the stainless-steel extrusion nozzle was replaced after material change. All test specimens were manufactured in a horizontal orientation. The parts were fabricated with 100% infill, a 45°/45° alternating infill pattern and 2 exterior perimeters.

There is evidence presented in scientific literature that the removal of oxygen from the printing chamber, for example by replacing it with inert gas [12], can lead to improved surface quality of printed parts. In order to determine whether this effect is present in the parts manufactured using the method described in this paper, the surface quality can be analyzed using atomic force microscopy. To analyze changes in the surface roughness, the printed parts made of ULTEM 1010 material were inspected using the NTEGRA Probe NanoLaboratory atomic force microscope. The parts were inspected on the lateral surface, in order to observe the quality of the surfaces at the interface between the successively deposited layers of material. The inspection was done along the longitudinal direction of the deposited filaments (Fig. 3).

In order to determine the mechanical characteristics of the parts printed under low vacuum, tensile tests were performed on a Hounsfield H10KT universal test machine (Fig. 4) with a maximum load capacity of 10 kN. The tests were performed with a pretension force of 5 N and a loading speed of 5 mm / min, at an ambient temperature of 24 °C and a humidity of 60%.

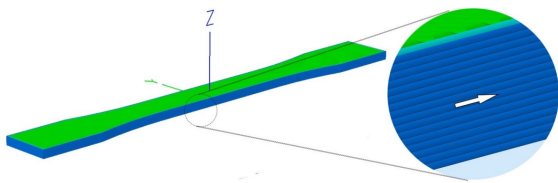


Fig. 3. Direction of atomic force scanning.

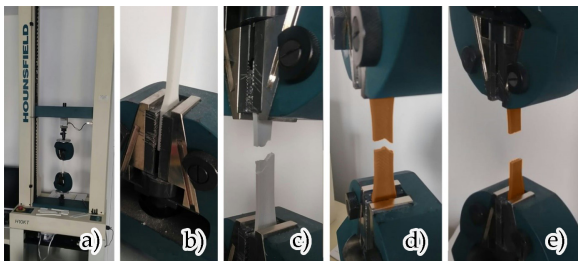


Fig. 4. Tensile stress testing: a – Hounsfield H10KT testing machine; b – 3D printed sample; c – tensile testing of ASA; d – tensile testing of PEI; e – uniform fracture of PEI specimen.

3. RESULTS

The dimensional accuracy of the specimens was measured after printing with an electronic caliper and it was found that there are no significant differences in the dimensions of parts printed in the vacuum chamber compared to those printed in the atmosphere at room temperature. In the case of two of the PEI specimens printed in atmospheric conditions, a partial detachment of the part from the printer bed was found, pointing to insufficient bed adhesion. All ASA specimens, as well as PEI vacuum-printed specimens had good bed adhesion. The results of the measurements with their standard errors are shown in Table 2.

Using the data recorded by the atomic force microscope, three-dimensional graphs (Fig. 5) were drawn for the inspected surfaces of the two types of parts.

The data regarding the surface quality of the parts were extracted using the NOVA software and can be found in Table 3.

Following this investigation, it can be concluded that the surfaces of the parts did not undergo significant changes following the variation of the environment in which they were printed.

Table 2

Dimensional accuracy of 3D printed samples

Material	Pressure	Length [mm]	Width [mm]	Height [mm]
ASA	1 atm	128.4±0.02	13.19±0.02	3.5±0.01
	15 Pa	128.34±0.07	13.18±0.02	3.51±0.01
PEI	1 atm	128.01±0.13	13.1±0.01	3.5±0.01
	15 Pa	128.36±0.02	13.05±0.03	3.49±0.01

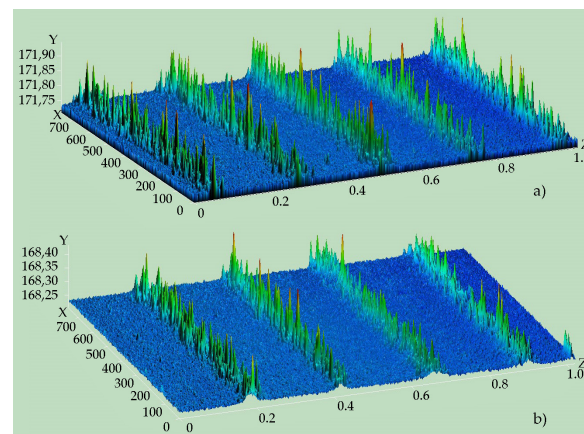


Fig. 5. 3D graphs of part surface roughness: a – surface roughness of PEI under atmospheric conditions; b – surface roughness of PEI in low vacuum

Table 3

Surface roughness for 3D printed ULTEM 1010

Printing environment	Ra roughness (µm)
Atmospheric pressure	6.50 ± 0.26
Low vacuum pressure	6.52 ± 0.21

During tensile strength testing, for all ASA specimens the tensile fracturing occurred along the longitudinal direction of deposited filaments. A similar way of fracturing is found in the case of PEI parts, with the exception of one of the low vacuum-printed specimens that fractured transversely (Fig. 4e), a sign that the deposited filaments had significantly higher adhesion.

For ASA specimens, the method presented in this paper did not produce significant changes of mechanical properties. The parts printed in low-vacuum suffered tensile failure at 38.8 MPa, compared to 38.4 MPa for the control group printed under atmospheric conditions (Fig. 6).

A similar result was obtained for stiffness, with the low-vacuum parts having a Young's Modulus of 2726 MPa compared to 2634 MPa for the control group. For PEI specimens, the changes were significant, the low-vacuum parts suffering tensile failure at 38.8 MPa, compared to 38.4 MPa for the control group printed under atmospheric conditions (Fig. 7). Stiffness also increased, with the low-vacuum parts having a Young's Modulus of 3370 MPa compared to 3160 MPa for the control group.

A discussion should also be made about the heat transfer in the printed parts, to see if the absence of air during the manufacturing process has a significant effect on the thermal behavior of the final part. Thus, a thermogram by Differential Scanning Calorimetry (DSC) was performed to highlight the thermal transitions in the

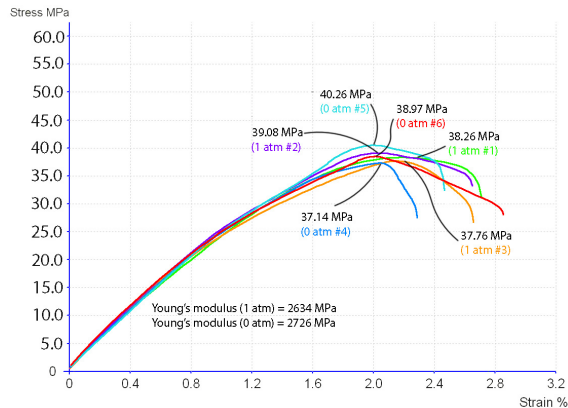


Fig. 6. Stress-strain curves for ASA parts during tensile strength testing.

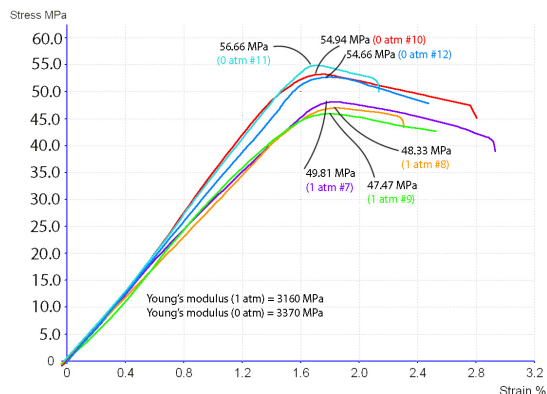


Fig. 7. Stress-strain curves for PEI (ULTEM 1010) parts during tensile strength testing.

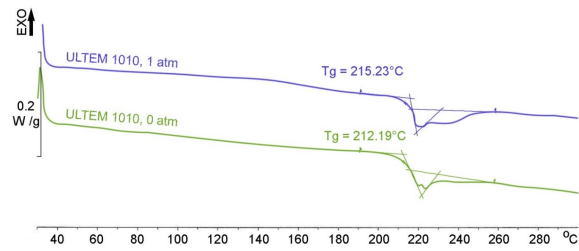


Fig. 8. Differential scanning calorimetry thermogram showing the glass transition for PEI parts (ULTEM 1010).

Table 4
Thermal transitions for 3D printed PEI (ULTEM 1010)

Specimen	T _g (°C)	T _{pk} (°C)
ULTEM 1010 / 1 atm	215.23 ± 0.30	217.09 ± 0.27
ULTEM 1010 / 0 atm	212.19 ± 0.29	219.94 ± 0.22

manufactured parts, namely the glass transition, which is of major importance in determining the temperature range in which the 3D printed parts can be used. Three test specimens were printed for each of the two cases: atmospheric printing and vacuum chamber printing. These were analyzed using a Shimadzu DTA-50 machine (Shimadzu Corp., Kyoto, Japan). The first heating cycle was 20–280 °C with a temperature rise rate of 5 °C/min, followed by cooling to 30 °C at a rate of 5 °C/min. The second heating cycle was 30–370 °C at a rate of 10 °C per minute. The analysis was performed in a nitrogen atmosphere at a flow rate of 85 mL/min. The thermal transitions that occurred in the second heating cycle are shown in Fig. 8, and the temperatures at which these transitions occurred are found in Table 4.

The glass transition for PEI parts printed under atmospheric conditions begins at $T_{g, 1atm} = 215.23$ °C and ends at $T_{pk, 1atm} = 218.02$ °C. These temperatures are in accordance with those found in the data sheet of the material, as well as in the literature. In the case of parts printed in a vacuum chamber, the glass transition starts at a slightly lower temperature $T_{g, 0atm} = 212.19$ °C and ends at $T_{pk, 0atm} = 220.24$ °C. A possible explanation for this phenomenon would be that the heat transfer in the reduced presence of internal air bubbles forming micro-voids. Since ULTEM 1010 is a material obtained from amorphous resin, there is no crystallization temperature, the degree of crystallization being 0. Also, the material does not have a melting point, but the fluidity of the material increases once the glass transition temperature is exceeded, reaching a flow rate of 17.8 g / 10 min under a load of 6.60 kg, at a temperature of 337 °C.

4. DISCUSSION AND CONCLUSIONS

In this paper, the feasibility of 3D printing thermoplastic materials with high extrusion temperature in a low-vacuum enclosure was investigated. Inside the build chamber, the phenomenon of thermal convection was eliminated by extracting air with a vacuum pump.

After designing and building a 3D printer with vacuum printing chamber, it was shown that the printing process is possible. Destructive and non-destructive test specimens with a simple geometry were successfully printed in this enclosure. Twelve ASTM D638 type I specimens were manufactured in atmospheric conditions and in the vacuum chamber of the 3D printer and were subjected to destructive tensile testing.

The dimensional accuracy of the manufactured parts was not significantly influenced by the absence of air in the enclosure, except for a very small number of specimens made of ULTEM 1010 material which partially detached from the raft structure due to internal thermal stresses when printed in atmospheric conditions. This defect occurred at the ends of the sample and did not affect sample structural integrity around the tensile failure section.

The results in Figs. 6 and 7 show that the impact of the absence of air is lower than expected in the case of ASA parts, given the similarity of the polymer to ABS and the precedents found in the literature. In the case of parts made of ULTEM 1010 polymer, the increases in strength are significant, on average the vacuum-printed specimens being 14% more resistant.

One direction to follow in the future is to establish a profile of process parameters that takes into account the geometry of the printed part in such a way that the heat transfer achieved by thermal conduction through the deposited material allows uniform cooling of the parts.

Indeed, from a technical point of view, the solution of using a vacuum chamber is more complex than certain alternatives, such as heating the enclosure or replacing the atmosphere with inert gas, but it also has certain advantages, such as eliminating the need for auxiliary materials (inert gas) and problems raised by their supply and storage. Also, in the absence of the thermal convection phenomenon, the temperature control in the case of the vacuum enclosure is more precise and does not depend on the dimensions of the side surfaces of the manufactured part, but only on the surface in contact with the printing bed or build platform. At the same time, there are applications in which the removal of oxygen prevents the oxidation of the material, such as in the case of filaments impregnated with metal powders. Additionally, better layer adhesion and elimination of internal micro-voids may lead to improved performance of printed parts in applications that require airtightness or sealing [13].

One approach of interest would be to combine the effect of a vacuum chamber with that of forced convection cooling, made possible by opening the valves of the vacuum chamber and allowing air to enter the enclosure. After cooling, the enclosure can be vacuumed again. This combination of effects would allow the manufacture of parts with more complex geometry, with structures such as overhangs.

REFERENCES

- [1] ResearchandMarkets.com, *Global Additive Manufacturing Market and Technology Forecast to 2028*, Market Report, 2020 ID 5144559.
- [2] H.-J. Steenhuis, L. Pretorius, *Consumer additive manufacturing or 3D printing adoption: An exploratory study*, J. Manuf. Technol. Manag., Vol. 27, 2016, pp. 990–1012.
- [3] S.F. Costa, F.M. Duarte, J.A. Covas, *Thermal conditions affecting heat transfer in FDM/FFE: A contribution towards the numerical modelling of the process*, Virtual Phys. Prototyp. Vol. 10 2015, pp. 35–46.
- [4] M.S. Priya, K. Naresh, R. Jayaganthan, R. Velmurugan, *A comparative study between in-house 3D printed and injection molded ABS and PLA polymers for low-frequency applications*, Mater. Res. Express. Vol. 6, 2019, 085345.
- [5] S.-H. Ahn, M. Montero, D. Odell, S. Roundy, P.K. Wright, *Anisotropic material properties of fused deposition modeling ABS*, Rapid Prototyp. J., Vol. 8, 2002, pp. 248–57.
- [6] J. Gardner, C.J. Stelter, E.A. Yashin, E.J. Siochi, *High Temperature Thermoplastic Additive Manufacturing Using Low-Cost, Open-Source Hardware*, Technical Report, 2016, NASA/TM-2016-219344.
- [7] J. Cantrell, S. Rohde, D. Damiani, R. Gurnani, L. DiSandro, J. Anton, A. Young, A. Jerez, D. Steinbach, C. Kroese, P. Ifju, *Experimental Characterization of the Mechanical Properties of 3D-Printed ABS and Polycarbonate Parts*. In: Yoshida S., Lamberti L., Sciammarella C. (eds) *Advancement of Optical Methods in Experimental Mechanics*, Vol. 3, 2016, Springer, Cham. pp 89–105.
- [8] F. Lederle, F.Meyer, G.-P. Brunotte, C. Kaldun, E.G. Hübner, *Improved mechanical properties of 3D-printed parts by fused deposition modeling processed under the exclusion of oxygen*, Prog. Addit. Manuf., Vol. 1, 2016, pp. 3–7.
- [9] A. Yardimci, T. Hattori, S. Guceri. *Thermal Analysis of Fused Deposition*, Rapid Prototyping Journal, 1997, pp. 689–698.
- [10] L.D. Jaffe, J.B. Rittenhouse, *Behavior of Materials in Space Environments*, Report No. 32–150 CIO, Jet Propulsion Laboratory.
- [11] ASTM International, *ASTM D638 – 14 Standard Test Method for Tensile Properties of Plastics*, 2014.
- [12] S.N.H. Mazlan, M.R.b. Alkahari, N.A. Maidin, F.R.b. Ramli, M.N. Sudin, G.D. Lim, I.S. Mohamad, *Influence of inert gas assisted 3D printing machine on the surface roughness and strength of printed components*, Proceedings of Mechanical Engineering Research Day, 2018, pp. 154–155.
- [13] E.G. Gordeev, S.A. Galushko, V.P. Ananikov. *Improvement of quality of 3D printed objects by elimination of microscopic structural defects in fused deposition modeling*, PLoS ONE, Vol. 13, No. 6, 2018, e0198370.